

J/ψ production in relativistic heavy ion collisions from a multi-phase transport model

Bin Zhang^a, C.M. Ko^b, Bao-An Li^a, Zi-Wei Lin^b, Subrata Pal^b

^a Department of Chemistry and Physics, Arkansas State University, State University, Arkansas 72467-0419, USA

^b Cyclotron Institute and Department of Physics, Texas A&M University, College Station, Texas 77843-3366, USA
(March 6, 2002)

Using A Multi-Phase Transport (AMPT) model, we study J/ψ production from interactions between charm and anti-charm quarks in initial parton phase and between D and \bar{D} mesons in final hadron phase of relativistic heavy ion collisions at the Relativistic Heavy Ion Collider (RHIC). Including also the inverse reactions of J/ψ absorption by gluons and light mesons, we find that the net number of J/ψ from the parton and hadron phases is smaller than that expected from the superposition of initial nucleon-nucleon collisions, contrary to the J/ψ enhancement predicted by the kinetic formation model. The production of J/ψ is further suppressed if one includes the color screening effect in the parton phase. We have also studied the dependence of J/ψ production on the charm quark mass and the effective charm meson mass.

25.75.Dw,24.10.Lx,24.10.Jv

I. INTRODUCTION

A central interest in modern nuclear physics is to produce and study the Quark-Gluon Plasma (QGP) predicted by the Quantum Chromodynamics (QCD) [1]. Studying the properties of the QGP and the deconfinement phase transition not only is important for understanding the QCD but also has astronomical implications [2]. Experiments at the Super Proton Synchrotron (SPS) involving collisions between heavy nuclei have shown that a large amount of energy is deposited around mid-rapidity, and the energy density may already be sufficiently large for the formation of the QGP during the initial stage of collisions [3]. More recent experiments at RHIC at Brookhaven National Laboratory, where the collision energy is much higher than at SPS, have also shown possible effects due to the formation of a partonic matter [4].

To find the signal for the Quark-Gluon Plasma in relativistic heavy ion collisions, Matsui and Satz proposed to study J/ψ production in these collisions [5]. Based on the fact that the effective potential between charm and anti-charm quarks changes in the QGP due to color screening effect, no bound states can be formed between them beyond a certain critical temperature, which is somewhat higher than the deconfinement temperature. As a result, J/ψ production is expected to be suppressed if the QGP is formed in heavy ion collisions. There are other possible mechanisms for J/ψ suppression [6–8] in heavy ion collisions, e.g., J/ψ can be destroyed by collisions with incoming nucleons or with gluons in the initial partonic matter [9,10] or with comoving hadrons in the hadronic matter [11–18]. The observed abnormal suppression of J/ψ in central Pb+Pb collisions at SPS may require the formation of the Quark-Gluon Plasma in these collisions [19,3].

For heavy ion collisions at RHIC energies, unlike in previous fixed target experiments at SPS, multiple pairs of charm-anti-charm quarks can be produced in one event, and these charm and anti-charm quarks can interact and produce the J/ψ [20]. This mechanism is the inverse reaction of J/ψ absorption by gluons. Using a kinetic approach, it was found that despite J/ψ dissociation due to color screening, this reaction is important in the quark-gluon plasma with temperatures between those for J/ψ dissociation and the deconfinement, and would lead to an enhanced production of J/ψ in heavy ion collisions at RHIC. A possible signal for QGP at RHIC has thus been changed from J/ψ suppression to J/ψ enhancement. The statistical fragmentation model [21–23], which has been extensively used for studying particle production in heavy ion collisions at SPS energies, predicts a comparable J/ψ production. The main assumption of this model is that J/ψ formed during hadronization of the QGP is in chemical equilibrium with charm mesons.

In the kinetic formation model, the heavy ion collision dynamics is treated schematically. For a more quantitative study of this new J/ψ production mechanism, we study J/ψ production from both the charm-anti-charm quark interactions and the charm-anti-charm meson interactions using the AMPT model [24–26]. In particular, we consider central ($b=0$) Au+Au collisions at the highest RHIC energy $\sqrt{s} = 200$ AGeV. With this dynamic transport model, we find that the net number of produced J/ψ from the parton and hadron phases is smaller than that expected from initial nucleon-nucleon collisions, contrary to the J/ψ enhancement predicted by the kinetic formation model. The production of J/ψ is further suppressed if one includes the color screening effect in the parton phase.

In Section II, we give a short description of the multi-phase transport model (AMPT). Results are presented in Section III for J/ψ production from the initial parton phase and the final hadron phase. In this section, we also

discuss the dependence of J/ψ production in the parton phase on the charm quark mass and in the hadron phase on the charm meson mass. Finally, we summarize the paper in Section IV.

II. MULTI-PHASE TRANSPORT MODEL AND J/ψ PRODUCTION MECHANISMS

The multi-phase transport model [24–26] that we use for the present study is a hybrid model based on three Monte-Carlo models for the three stages of relativistic heavy ion collisions, i.e., the Heavy Ion Jet Interaction Generator (HIJING) [27,28] for the initial conditions, Zhang’s Parton Cascade (ZPC) [29] for the parton evolution, and A Relativistic Transport (ART) model [30,31] for the hadron evolution. In the HIJING model, nucleons are distributed according to the Woods-Saxon distribution. The parton distribution in a nucleon is adjusted according to the transverse position of the nucleon and a shadowing function based on the Mueller-Qiu parton recombination mechanism [32]. These partons undergo hard or semi-hard collisions and generate an initial parton system after the passage of two colliding nuclei. HIJING provides the momentum space information of the partons produced in the hard or semi-hard collisions. The formation time of a parton is generated according to the Gyulassy-Wang model of parton coherent production [33]. The position of a physical parton is then obtained from the position of its parent nucleon by adding a displacement given by its velocity times the formation time. The resulting parton phase space distribution is used as the initial conditions for starting the ZPC parton evolution. In the present version of the ZPC model, only elastic gluon-gluon scattering are included with a cross section of 3 mb, which is consistent with the estimated average screening mass in the partonic matter formed in the collisions. When the partonic matter stops interacting, partons are connected back with their parent nucleons, which also suffer soft interactions through string excitations. The Lund fragmentation model [34] is then called from the HIJING model to convert these wounded nucleons into hadrons. These hadrons become physical after a formation time given by the average freeze-out proper time of partons in a string plus an additional 0.7 fm/c to account for the time that is required for producing quark-anti-quark pairs. The ensuing hadron evolution is modeled by the ART model that takes into account interactions among nucleons, anti-nucleons, mesons, and resonances. For a better description of experimental hadron spectra, the original ART model has been improved by including the K^* meson interactions, the anti-nucleon production, and the ρ meson interactions.

We have previously used this multi-phase transport model to study the suppression of primarily produced J/ψ in heavy ion collisions at RHIC [35]. These J/ψ ’s are produced in nucleon-nucleon collisions during the initial passage of two colliding nuclei. Because of color screening, these J/ψ ’s are not physical ones but correlated pairs of charm-anti-charm quarks close in phase space. They become physical J/ψ ’s if they remain close when the partonic matter cools below the J/ψ dissociation temperature. Otherwise, they will combine with nearby light quarks to form charm mesons at hadronization. Gluons can also destroy the phase space correlation between the charm quark and anti-quark pairs and hence destroy the J/ψ . It was found that finite space size and lifetime have significant effects on J/ψ suppression, and different mechanisms lead to different suppression factors. Also, the dependence of J/ψ suppression on the size of colliding nuclei was shown to be useful for differentiating the different suppression mechanisms. Similar results have also been obtained in other studies [36,37].

In the present study, we include the reactions of J/ψ production from charm-anti-charm quark interactions in the parton phase and from charm meson interactions in the hadron phase. As the primary J/ψ number is much smaller than the number of other particles participating in the equilibration, primary J/ψ evolution won’t affect secondary J/ψ production. We do not include primary J/ψ ’s in the following calculations.

The charm and anti-charm quarks are generated from the PYTHIA model [38], with a cross section of 350 μb for producing a pair of charm-anti-charm pair in a nucleon-nucleon collision. This cross section does not include nuclear shadowing effect of gluons, so the present study gives an upper bound for charm meson and J/ψ production in heavy ion collisions. In the partonic stage of heavy ion collisions, J/ψ ’s are then produced from charm-anti-charm quark interactions through the reaction $c + \bar{c} \rightarrow J/\psi + g$. The J/ψ can also be destroyed by gluons through the reaction $g + J/\psi \rightarrow c + \bar{c}$. We further include the dissociation of J/ψ due to color screening in the partonic matter. To treat this process, we follow the method used in Ref. [35] by introducing a critical radius in the transverse plane of a heavy ion collision, within which the parton energy density is larger than the critical energy density for J/ψ dissociation by color screening and the J/ψ thus cannot be formed. The critical radius decreases as the partonic matter expands. The time evolution of this critical radius in Au+Au collisions at $\sqrt{s} = 200$ AGeV has been parameterized in Ref. [35]. In addition to producing the J/ψ , charm and anti-charm quarks also undergo elastic scattering with gluons. This elastic cross section is taken to be 3 mb in the present study.

After partons stop interacting, charm and anti-charm quarks are converted to D and \bar{D} mesons. This conversion is carried out using a delta function fragmentation scheme. In this approach, the momentum of a charm meson is taken to be the same as the momentum of its parent charm quark. A formation time of 1 fm/c is also introduced in

combining the charm quark with a nearby light quark. Because of the large mass of charm quark, the delta function fragmentation scheme gives a reasonable description of charm quark fragmentation in hadron reactions. For simplicity, we do not differentiate between D mesons and D^* mesons. Instead, we vary the D meson mass to study the influence of different production thresholds for J/ψ production from charmed hadrons.

In the hadronic phase, D and \bar{D} mesons can interact to produce a J/ψ and a light meson through the reaction $D\bar{D} \rightarrow J/\psi M$, where M denotes a light meson. The J/ψ can also be destroyed by light mesons through the inverse reaction $J/\psi M \rightarrow D\bar{D}$. We only include reactions that involve π mesons or ρ mesons as they are the most abundant ones in the nearly baryon free matter formed in heavy ion collisions at RHIC. The cross section for light meson destruction of J/ψ is taken to be 3 mb as in previous transport study at SPS energies [13–18]. This cross section is consistent with those from recent theoretical studies based on effective hadronic Lagrangians [39–41], the quark-exchange model [42], and the QCD sum rules [43]. The cross section for the inverse reaction of J/ψ production from D mesons is calculated according to the detailed balance relation. As we do not differentiate between D mesons and D^* mesons, the spin and isospin degrees of freedom for both D and D^* mesons are used in evaluating the inverse reaction cross section. This is equivalent to including all possible combination of D and D^* states. We will vary the D meson mass to study the effect due to changing J/ψ production threshold.

In earlier studies based on kinetic models [44], J/ψ production from the hadron phase of relativistic heavy ion collisions was found to be important only at LHC [44,45] but not at RHIC as the cross section for $D\bar{D} \rightarrow J/\psi M$ used in these studies was smaller than that used in present study.

Although multiple pairs of charm quarks are expected to be produced in each Au+Au collision, the number of charm quarks is small compared with other particles. For example, the rapidity density of charm quark pairs is about 1.5 at $\sqrt{s} = 200$ AGeV. The expected number of J/ψ per event is even much smaller. To obtain sufficient statistics for J/ψ production, charm particles and the J/ψ are treated in the transport model by the perturbative method [46,47], i.e., neglecting their effects on heavy ion collision dynamics. This method has been used extensively for studying rare particle production in heavy ion collisions at low energies. Explicitly, we include many charm quark events from primary nucleon-nucleon interactions in the evolution of partons from a single HIJING event. However, only charm quarks from the same event are allowed to interact among themselves, and the usual method of treating binary collisions in transport models is used in treating these collisions. For collisions between charm and uncharm particles, we keep their effects on the charm particles but neglect those on the uncharm particles. In this way, the dominant computation time for the interactions between uncharm particles remains the same as for a single charm event. Since there are much more uncharm particles than charm particles, e.g., about 300 gluons verse about 3 charm and anti-charm quarks per unit rapidity, neglecting the effects of charm particles on the heavy ion collision dynamics is expected to be a very good approximation.

III. RESULTS

A. J/ψ production in parton phase

We first study J/ψ production in the parton phase. Unless otherwise indicated, the rates and numbers in the following are all rapidity densities averaged with $|y| < 1$. Fig. 1 gives the time evolution of the production and destruction rates per unit rapidity for J/ψ 's with $|y_{J/\psi}| < 1$. Also shown is the rate per unit rapidity for collisions between charm and anti-charm quarks which would have produced the J/ψ in the absence of color screening effect. These unsuccessful collisions mainly occur before 0.5 fm/c when most partonic matter have effective temperatures above the J/ψ dissociation temperature. The screening effect largely diminishes after 1 fm/c when the parton density decreases due to expansion. At this time, the J/ψ production rate starts to increase quickly, and this is followed by an increase of the J/ψ destruction rate. After reaching their peak values, both the production and destruction rates decrease and become comparable at about 4 fm/c.

To see more clearly the relative importance of J/ψ production and destruction in the parton phase, we show in Fig. 2 the time evolution of the number of produced J/ψ and the number of destructed J/ψ as well as the net J/ψ number. The number of J/ψ saturates at about 3 fm/c. It decrease slowly afterwards as the production and destruction rates become comparable as shown in Fig. 1.

In the absence of color screening effect, collisions between charm and anti-charm quarks in the partonic matter that is above the J/ψ dissociation temperature can also produce the J/ψ . This leads to a very high J/ψ production rate before 0.5 fm/c as shown in Fig. 3. The J/ψ destruction rate during this time also reaches its peak value of about 1/3 of the maximum production rate. In contrast to the case including color screening effect, the production and destruction rates become comparable already at about 0.5 fm/c. As shown in Fig. 4, these result in a much faster increase in the numbers of produced and destructed J/ψ , and an earlier peaking in the net J/ψ number than in the

case with color screening effect. Since the destruction rate after 0.5 fm/c is still slightly larger than the production rate, the net J/ψ number slowly decreases from its maximum value of about 0.003 to a final value of about 0.0014 per event. This number is about a factor of two larger than the final net J/ψ number for the case with color screening effect, which is about 0.0007 per event.

The number of J/ψ expected from primary nucleon-nucleon collisions in Au+Au central collisions can be estimated from the J/ψ production cross section in pp collisions. The cross section per unit rapidity at $\sqrt{s} = 200$ AGeV is $0.63 \mu\text{b}$ [48]. Using the nuclear overlap function $T_{Au+Au}(b=0) = 30 \text{ mb}^{-1}$, we expect 0.019 J/ψ per unit rapidity to be produced in Au+Au central collisions. This is much larger than the predictions of 0.0007 and 0.0014 from the dynamical multi-phase transport model. Our study thus predicts a suppression of J/ψ production in the parton phase of heavy ion collisions at RHIC, and this is opposite to the enhancement predicted by the kinetic formation model.

B. J/ψ production in hadron phase

In hadronic matter, the threshold for J/ψ production is reduced in comparison with that in the partonic matter as the D meson mass is larger than the charm quark mass. This threshold effect is expected to compensate for the lower charm density in the hadron phase than in the parton phase. To demonstrate this threshold effect, we vary the D meson mass in studying J/ψ production in the hadronic matter. Fig. 5 shows the time evolution of J/ψ production and destruction rates per unit rapidity in the hadron phase for different D meson masses. These results are obtained with the color screening effect included in the initial parton phase. The upper panel is for $m_D = 1.70$ GeV, which is smaller than the D meson mass in vacuum. We use this smaller mass because theoretical studies have shown that the D meson mass may be reduced in medium [49–52]. The middle panel is for $m_D = 1.87$ GeV, which is the D meson mass in vacuum. Here, we treat D^* meson mass as D meson mass, and the results are thus a lower bound for J/ψ production. The lower panel is for $m_D = 2.01$ GeV, which is the D^* mass in vacuum. Treating D meson mass as D^* meson mass in this case then gives an upper bound for J/ψ production. The destruction rates for all three D meson masses are seen to have similar magnitude. For the production rate, it is larger for larger D meson masses.

In Fig. 6, we show the time evolution of the numbers of produced and destructed J/ψ together with that of the net J/ψ number. For $m_D = 1.87$ GeV and $m_D = 2.01$ GeV, the number of produced J/ψ is always greater than the number of destructed J/ψ , leading to a net production of J/ψ from the hadron phase of relativistic heavy ion collisions. With increasing D meson mass, the destructed J/ψ number increases slightly while the produced J/ψ increases drastically. For $m_D = 1.70$ GeV, the produced and destructed J/ψ numbers are about equal, and the final net J/ψ number is thus about the same as that from the parton phase. On the other hand, for $m_D = 2.01$ GeV, the final J/ψ number equals approximately the number of produced J/ψ from the hadron phase. The final J/ψ number reflects essentially the one produced from the hadron phase.

Quantitatively, the final net number of J/ψ per unit rapidity averaged over $|y_{J/\psi}| < 1$ is about 0.0007 per event for $m_D = 1.70$ GeV and increases to 0.0019 for $m_D = 1.87$ GeV and to 0.0053 for $m_D = 2.01$ GeV. The time evolution of the net J/ψ number in the three cases are similar as it is largely determined by the heavy ion collision dynamics. The J/ψ number saturates at about 15-20 fm/c, which is about the lifetime of the hadronic matter.

The results for neglecting the color screening effect in the initial parton phase are shown in Fig. 7 for time evolution of the J/ψ production and destruction rates and in Fig. 8 for the time evolution of the numbers of produced and destructed J/ψ as well as the net J/ψ number. Although there are more J/ψ 's destructed in the hadronic matter, particularly for $m_D = 1.70$ GeV where the number of destructed J/ψ is even larger than the number of produced J/ψ in the hadron phase, the final J/ψ number is larger than in the case with color screening in the parton phase. Their numbers are 0.0010, 0.0024, and 0.0057 for $m_D = 1.70, 1.87,$ and 2.01 GeV, respectively.

C. discussions

The relative importance of J/ψ production from the parton and hadron phases is more clearly seen in Fig. 9, where we show the number of produced J/ψ per unit rapidity with $|y_{J/\psi}| < 1$ as a function of the D meson mass. The results with color screening in the parton phase are shown by open circles for production from the parton phase and filled circles for the final J/ψ number including production from the hadron phase. Without color screening in the parton phase, the corresponding results are given by diamonds. As expected, including color screening effect leads to a decrease in the final J/ψ number. As the D meson mass increases, the final J/ψ yield increases strongly due to production from the hadron phase, and the effect due to color screening becomes less important. The results using $m_D = 2.01$ GeV give the upper bound for J/ψ production while those using $m_D = 1.87$ GeV give a lower bound. We

note again that the net effect of a reduced D meson mass of $m_D = 1.70$ GeV is the destruction of J/ψ 's produced from the parton phase in the absence of color screening.

Part of increased production of J/ψ in midrapidity when the effective D meson mass increases is due to increase in the charm meson rapidity density during hadronization. This is shown in Fig. 10, where we give the midrapidity densities of charm quarks before (lower dashed line) and after (lower solid line) parton evolution as well as of charm mesons before (upper dashed line) and after (upper solid line) hadron evolution. During parton evolution, the rapidity density of charm and anti-charm quarks decreases slightly due to collisions with gluons. Hadronization increases the midrapidity density of resulting charm mesons, and its effect increases with increasing charm meson effective mass. The midrapidity density of D and \bar{D} mesons is seen to increase by 8% when m_D increases from 1.70 GeV to 2.01 GeV. However, this would lead to at most 20% increase in the J/ψ midrapidity density and cannot account for the more than factor of 5 increase in J/ψ production shown in Fig. 9. The dominant effect for such a larger increase is thus due to the reduced threshold for J/ψ production when D meson mass increases.

The charm quark mass strongly influences the number of J/ψ produced from the parton phase. Fig. 11 shows the J/ψ rapidity density as a function of the charm quark mass. To get the upper limit of J/ψ production, the D meson mass is set to be 2.01 GeV and color screening is not included. The J/ψ number increases by a factor of 72% when the charm quark mass increases from the value 1.35 GeV used in PYTHIA to 1.5 GeV used in the constituent quark model. If the charm quark mass is taken to be 1.8 GeV, we observe about a factor of 4 increase in J/ψ production from the parton phase compared with the $m_c = 1.35$ GeV case.

In the kinetic model approach of Ref. [20], the midrapidity density of charm quarks in Ref. [20] is about 2.5 because the largest rapidity range for about 10 pairs of charm and anti-charm quarks is 4 in that study. This is larger than that shown in Fig. 10, which is about $3.48/2=1.74$. Since J/ψ production is roughly proportional to the square of the number of charm quarks, this can lead to about a factor of 2 difference between our results and those from Ref. [20]. On the other hand, the cross section we use for J/ψ production from the charm and anti-charm quarks is about a factor two larger than the peak value used in the kinetic model. The effects due to different midrapidity charm quark densities and J/ψ production cross sections in these two studies are thus largely cancelled out. The different conclusions of J/ψ suppression in our study and J/ψ enhancement in the kinetic approach are results of different heavy ion collision dynamics used in the two studies. In our approach, the parton phase is generated from the mini-jet gluons from initial hard and semi-hard collisions between nucleons and is evolved using the transport model. In the kinetic approach, an equilibrated quark-gluon plasma is assumed to be formed in the initial stage and later expands according to the 1-D Bjorken hydrodynamical model [53]. Further studies are required to determine the validity of these predictions.

IV. SUMMARY

In this paper, we have studied the effects due to interactions between charm and anti-charm quarks in the initial parton phase and between charm mesons in the final hadron phase on J/ψ production in central Au+Au collisions at RHIC. Using a multi-phase transport model, we find that because of the high density of charm quarks at early times, the J/ψ can be produced from the interactions of charm quarks. This is consistent with the conclusion of the kinetic formation model. However, the more realistic space-time evolution given by the transport model leads to an overall suppression of J/ψ particles in the parton phase, instead of an enhancement predicted by the kinetic model.

We have also shown that J/ψ can be produced in the hadron phase at RHIC. This is due to the large D meson mass compared with charm quark mass. Although we have not taken into account parton-hadron interactions in the multi-phase model, both parton phase and hadron phase can exist in the same space-time region. This allows the production of J/ψ 's in the mixed phase. At RHIC energies, the multi-phase model shows that hadron medium effect may lead to a net destruction of the J/ψ produced in the parton phase. In addition, color screening is shown to have significant effect on the final J/ψ yield.

In the present study, we have not included the effect due to gluon shadowing [54], which would reduce the charm quark and J/ψ numbers. As the multi-phase transport model predicts an overall suppression of the directly produced J/ψ , including gluon shadowing effect on the initial charm quark distribution will not change qualitatively the conclusion from the multi-phase model. Also, J/ψ from decays of ψ' or χ_c was not considered in our study. The contribution from primary ψ' or χ_c to final J/ψ are negligible due to their large destruction cross sections compared with that for J/ψ . Although the production cross sections for ψ' and χ_c from charm quark interactions and charm meson interactions are expected to be larger than those for J/ψ , the thresholds for these reactions are also higher. In particular, the statistical fragmentation model [21,22] indicates that the feeddown should be small for central collisions. We thus expect that our conclusion of J/ψ suppression in heavy ion collisions at RHIC will not be qualitatively modified.

ACKNOWLEDGMENTS

We thank P. Braun-Munzinger, M. Gyulassy, J. Kapusta, S. Pratt, R. Rapp, A.T. Sustich, C. Teal, R. Thews, W. Weise, and I. Zahed for helpful discussions. We also thank the Parallel Distributed System Facility at the National Energy Research Scientific Computer Center for providing computer resources. This work is supported by the U.S. National Science Foundation under Grant No. 0088934 and Grant No. 0098805, the Arkansas Science and Technology Authority under Grant No. 01-B-20, the Welch Foundation under Grant No. A-1358, and the Texas Advanced Research Program under Grant No. FY99-010366-0081.

- [1] F. Wilczek, Phys. Today **53**, 22 (2000).
- [2] B. Müller, Rep. Prog. Phys. **58**, 611 (1995).
- [3] U. Heinz and M. Jacob, e-Print archive: nucl-th/0002042.
- [4] Proceedings of 15th International Conference on Ultra-Relativistic Nucleus-Nucleus Collisions (Quark Matter 2001), Nucl. Phys. **A698**.
- [5] T. Matsui and H. Satz, Phys. Lett. B **178**, 416 (1986).
- [6] E772 Collaboration (D.M. Alde *et al.*), Phys. Rev. Lett. **66**, 133 (1991).
- [7] E866/NuSea Collaboration (M. Leitch *et al.*), Phys. Rev. Lett. **84**, 3256 (2000).
- [8] NA 50 Collaboration (M.C. Abreu *et al.*), Phys. Lett. B **410**, 337 (1997).
- [9] E.V. Shuryak, Sov. J. Nucl. Phys. **28**, 408 (1979).
- [10] X.M. Xu, D. Kharzeev, H. Satz, and X.N. Wang, Phys. Rev. C **53**, 3051 (1996).
- [11] S. Gavin and R. Vogt, Phys. Rev. Lett. **78**, 1006 (1997).
- [12] A. Capella, E.G. Ferreira, and A.B. Kaidalov, Phys. Rev. Lett. **85**, 2080 (2000).
- [13] C. Spieles, R. Vogt, L. Gerland, S.A. Bass, M. Bleicher, L. Frankfurt, M. Strikman, H. Stöcker, and W. Greiner, Phys. Lett. B **458**, 137 (1999).
- [14] C. Spieles, R. Vogt, L. Gerland, S.A. Bass, M. Bleicher, H. Stöcker, and W. Greiner, Phys. Rev. C **60**, 054901 (1999).
- [15] W. Cassing and C.M. Ko, Phys. Lett. B **396**, 39 (1997).
- [16] J. Geiss, C. Greiner, E.L. Bratkovskaya, W. Cassing, and U. Mosel, Phys. Lett. B **447**, 31 (1999).
- [17] D.E. Kahana, S.H. Kahana, Phys. Rev. C **59**, 1651 (1999).
- [18] B.H. Sa, A. Tai, H. Wang, and F.H. Liu, Phys. Rev. C **59**, 2728 (1999).
- [19] D. Kharzeev, C. Lounrenco, M. Nardi, and H. Satz, Zeit. Phys. C **74**, 307 (1997).
- [20] R. Thews, M. Schroedter, and J. Rafelski, Phys. Rev. C **63**, 054905 (2001).
- [21] P. Braun-Munzinger and J. Stachel, Phys. Lett. B **490**, 196 (2000).
- [22] P. Braun-Munzinger, Nucl. Phys. **A690**, 119 (2001).
- [23] L. Grandchamp and R. Rapp, e-Print archive: hep-ph/0103124.
- [24] B. Zhang, C.M. Ko, B.A. Li, and Z.W. Lin, Phys. Rev. C **61**, 067901 (2000).
- [25] Z.W. Lin, S. Pal, C.M. Ko, B.A. Li, and B. Zhang, Phys. Rev. C **64**, 011902 (2001).
- [26] Z.W. Lin, S. Pal, C.M. Ko, B.A. Li, and B. Zhang, Nucl. Phys. **A698**, 375c (2002).
- [27] X.N. Wang and M. Gyulassy, Phys. Rev. D **44**, 3501 (1991).
- [28] M. Gyulassy and X.N. Wang, Comput. Phys. Commun. **83**, 307 (1994).
- [29] B. Zhang, Comput. Phys. Commun. **109**, 193 (1998).
- [30] B.A. Li and C.M. Ko, Phys. Rev. C **52**, 2037 (1995).
- [31] B.A. Li, A.T. Sustich, B. Zhang, and C.M. Ko, Int. J. of Mod. Phys. **10**, 267 (2001).
- [32] A. Mueller and J. Qiu, Nucl. Phys. **B286**, 427 (1986).
- [33] M. Gyulassy and X.N. Wang, Nucl. Phys. **B420**, 583 (1994).
- [34] B. Andersson, G. Gustafson, G. Ingelman, and T. Sjöstrand, Phys. Rep. **97**, 31 (1983).
- [35] B. Zhang, C.M. Ko, B.A. Li, Z.W. Lin, and B.H. Sa, Phys. Rev. C **62**, 054905 (2000).
- [36] R. Vogt, Nucl. Phys. **A661**, 250c (1999).
- [37] W. Cassing, E.L. Bratkovskaya, S. Juchem, Nucl. Phys. **A674**, 249 (2000).
- [38] T. Sjöstrand, Comput. Phys. Commun. **82**, 74 (1994).
- [39] K.L. Haglin, Phys. Rev. C **61**, 031902 (2000).
- [40] Z.W. Lin and C.M. Ko, Phys. Rev. C **62**, 034903 (2000); W. Liu, C. M. Ko, and Z.W. Lin, *ibid.* **65** 015203 (2002).
- [41] A. Sibirtsev, K. Tsushima, and A.W. Thomas, Phys. Rev. C **63**, 044906 (2001).
- [42] C.Y. Wong, T. Barnes, and E.S. Swanson, Phys. Rev. C **62** 045201 (2000); **64** 014903 (2002); C.Y. Wong, T. Barnes, E.S. Swanson, and H.W. Crater, e-Print archive: nucl-th/0112023.

- [43] F. S. Navarra, M. Nielsen, R. S. Marques de Carvalho, and G. Krein, nucl-th/0105058.
[44] C.M. Ko, X.N. Wang, B. Zhang, and X.F. Zhang, Phys. Lett. B **444**, 237 (1998).
[45] P. Braun-Munzinger and Krzysztof Redlich, Eur. Phys. J. C **16**, 519 (2000).
[46] J. Randrup and C.M. Ko, Nucl. Phys. **A343**, 519 (1980).
[47] X.S. Fang, C.M. Ko, and Y.M. Zheng, Nucl. Phys. **A556**, 499 (1993).
[48] P. Gavai, D. Kharzeev, H. Satz, G.A. Schuler, K. Sridhar, and R. Vogt, Int. J. Mod. Phys. **A10**, 3043 (1995).
[49] K. Tsushima, D.H. Lu, A.W. Thomas, K. Saito, and R.H. Landau, Phys. Rev. C **59**, 2824 (1999).
[50] A. Hayashigaki, Phys. Lett. **B487**, 96 (2000).
[51] W. Weise, Proceedings of Hirschegg'01: Structure of Hadrons: 29th International Workshop on Gross Properties of Nuclei and Nuclear Excitations.
[52] A. Sibirtsev, K. Tsushima, K. Saito, and A.W. Thomas, Phys. Lett. **B484**, 23 (2000).
[53] J.D. Bjorken, Phys. Rev. D **27**, 140 (1983).
[54] N. Hammon, L. Gerland, H. Stöcker, W. Greiner, Phys. Rev. C **59**, 2744 (1999).

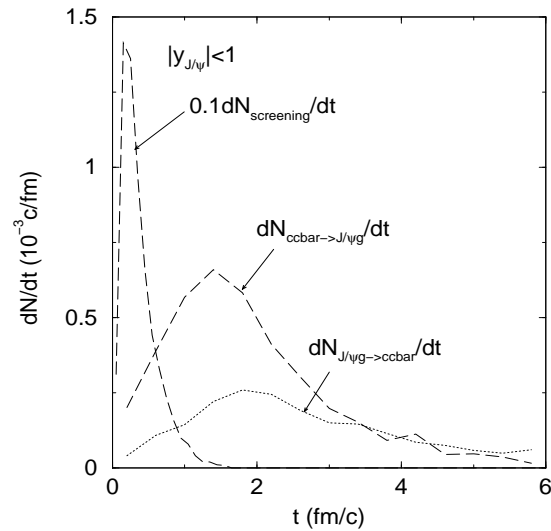


FIG. 1. Time evolution of the production rate (dashed line) and the destruction rate (dotted line) per unit rapidity for J/ψ with $|y_{J/\psi}| < 1$ in the parton phase with the color screening effect. The thin dashed line denotes the collision rate per unit rapidity of charm and anti-charm quarks which would have produced the J/ψ if color screening effect is absent.

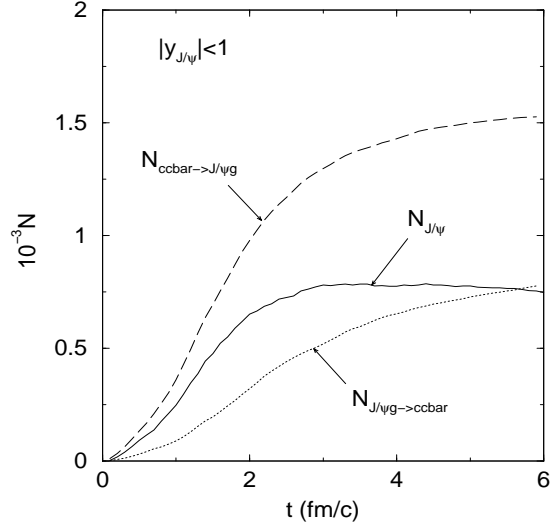


FIG. 2. Time evolution of produced number (dashed line), destroyed number (dotted line), and net number (solid line) per unit rapidity for J/ψ with $|y_{J/\psi}| < 1$ in the parton phase with the color screening effect.

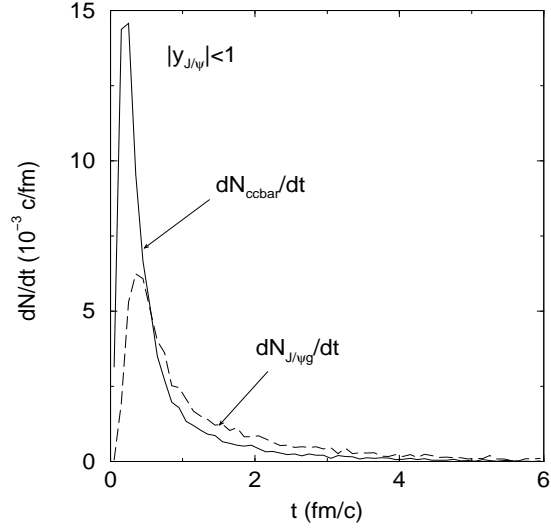


FIG. 3. Time evolution of the production rate (solid line) and the destruction rate (dashed line) per unit rapidity for J/ψ with $|y_{J/\psi}| < 1$ in the parton phase without color screening effect.

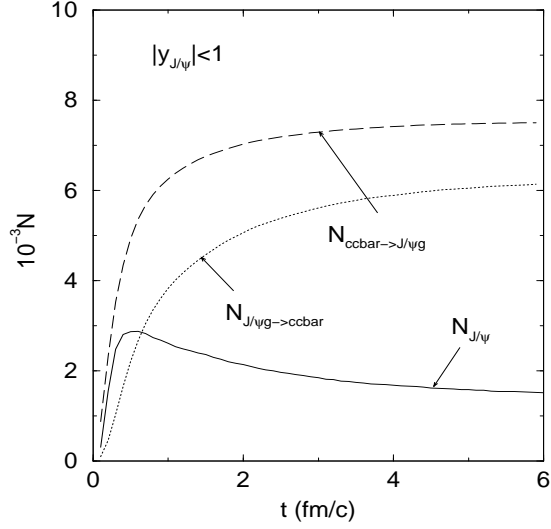


FIG. 4. Time evolution of produced number (dashed line), destroyed number (dotted line), and net number (solid line) per unit rapidity for J/ψ with $|y_{J/\psi}| < 1$ in the parton phase without color screening effect.

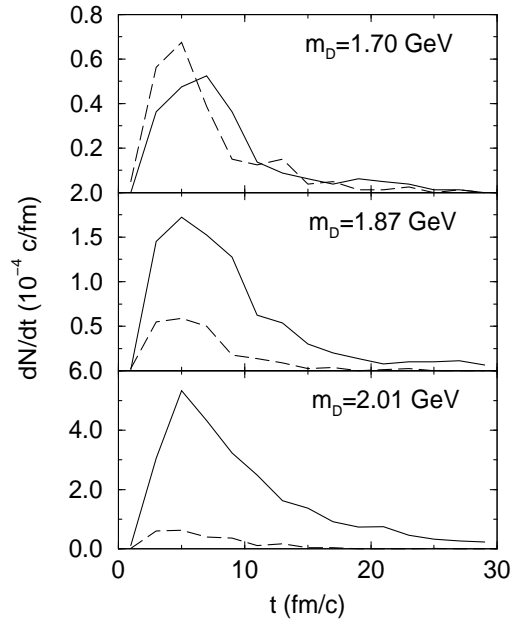


FIG. 5. Time evolution of the production rate (solid line) and the destruction rate (dashed line) per unit rapidity for J/ψ with $|y_{J/\psi}| < 1$ from the hadron phase for three values of D meson mass. Color screening effect is included in the initial parton phase.

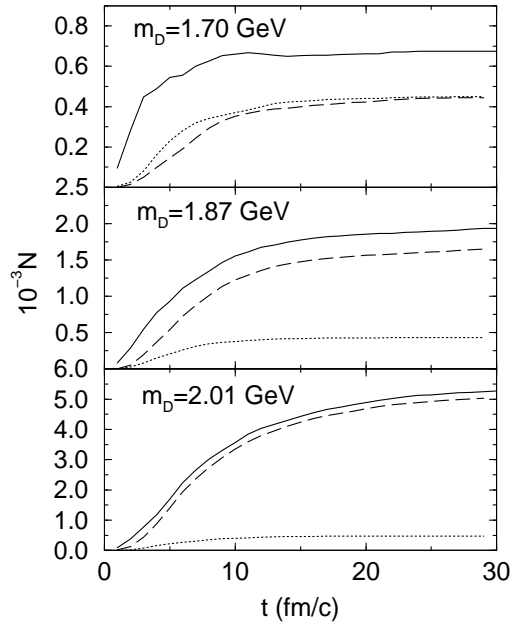


FIG. 6. Time evolution of produced number (dashed line), destructed number (dotted line), and net number (solid line) per unit rapidity for J/ψ with $|y_{J/\psi}| < 1$ for three values of D meson mass. Color screening effect is included in the initial parton phase.

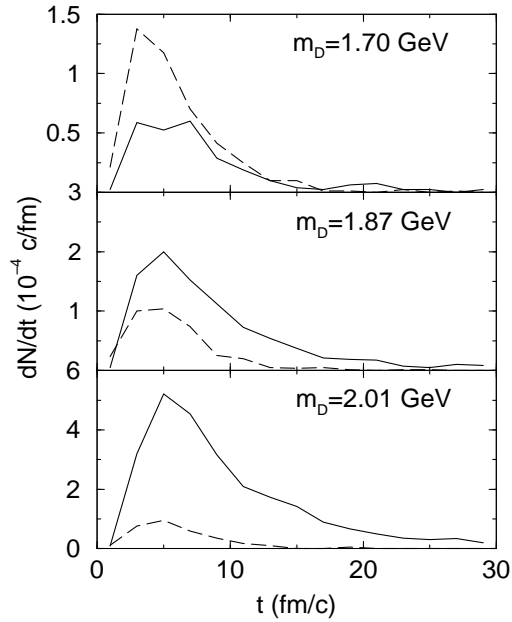


FIG. 7. Time evolution of the production rate (solid line) and the destruction rate (dashed line) per unit rapidity for J/ψ with $|y_{J/\psi}| < 1$ from the hadron phase for three values of D meson mass. Color screening effect is not included in the initial parton phase.

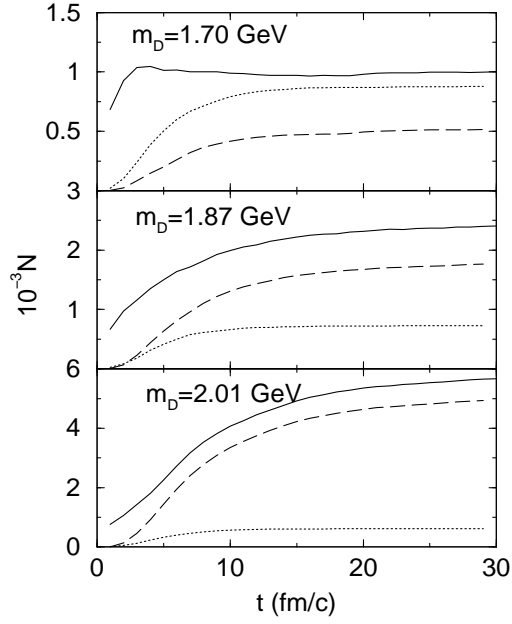


FIG. 8. Time evolution of produced number (dashed line), destructed number (dotted line), and net number (solid line) per unit rapidity for J/ψ with $|y_{J/\psi}| < 1$ in the hadron phase for three values of D meson mass. Color screening effect is not included in the initial parton phase.

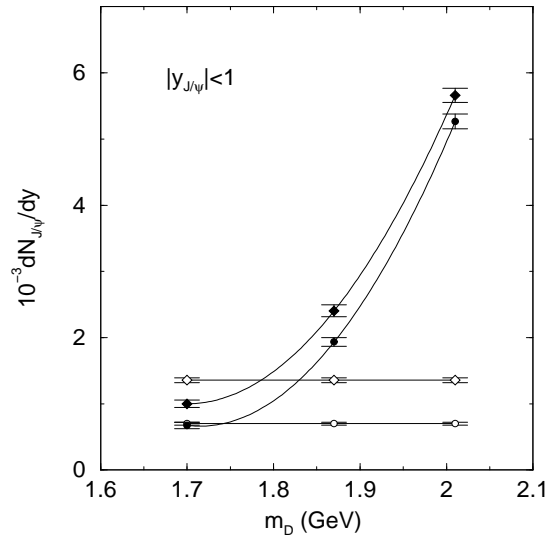


FIG. 9. Number of produced J/ψ per unit rapidity with $|y_{J/\psi}| < 1$ as a function of D meson mass. Open symbols are for production in the parton phase while filled symbols are for the final number including production from the hadron phase. Circles and diamonds are, respectively, the results with and without color screening in the parton phase. Error bars are statistical.

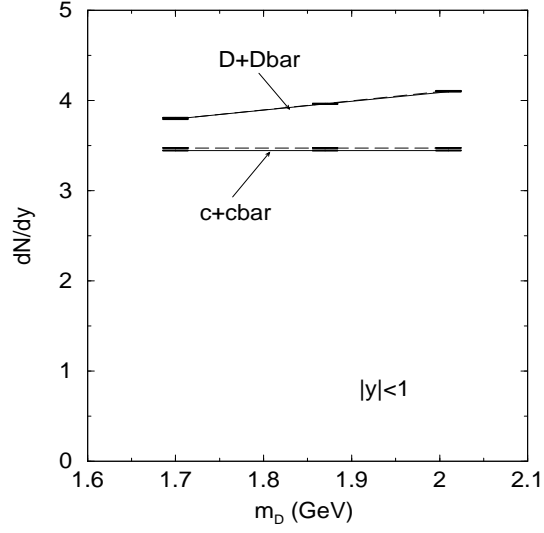


FIG. 10. Midrapidity densities of charm quarks before (lower dashed line) and after (lower solid line) parton evolution as well as of charm mesons before (upper dashed line) and after (upper solid line) hadron evolution.

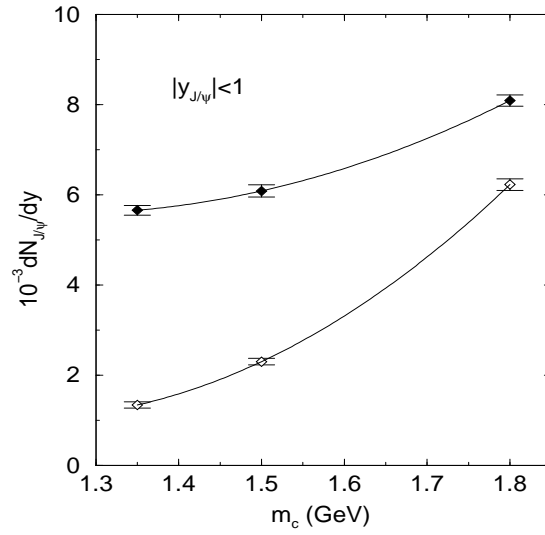


FIG. 11. Midrapidity density of J/ψ as a function of the charm quark mass for the production in the parton phase (open diamonds) and the final number including the production in the hadron phase (filled diamonds). Error bars are statistical.